Phase diagram in an external magnetic field beyond a mean-field approximation

V. Skokov

Phys. Rev. D **85**, 034026 — Published 14 February 2012

DOI: 10.1103/PhysRevD.85.034026

BNL-96687-2011-JA

Phase diagram in an external magnetic field beyond a mean-field approximation

V. Skokov[1, *]

[1] *Physics Department, Brookhaven National Laboratory, Upton, NY 11973, USA*

The phase structure of the Polyakov loop-extended chiral quark–meson model is explored in a nonperturbative approach, beyond a mean-field approximation, in the presence of a magnetic field. We show that by including meson fluctuations one cannot resolve the qualitative discrepancy on the dependence of the crossover transition temperature in a non-zero magnetic field between effective model predictions and recent lattice results (arXiv:1111.4956).We compute the curvature of the crossover line in the $T - \mu_B$ plane at a non-zero magnetic field and show that the curvature increases with increasing magnetic field. On the basis of QCD inequalities, we also argue that, at least in the large N_c limit, a chiral critical end point and, consequently, a change from crossover to a first-order chiral phase transition are excluded at zero baryon chemical potential and non-zero magnetic field.

PACS numbers: 24.85.+p,21.65.-f,25.75.-q,24.60.-k

I. INTRODUCTION

The phase diagram of strongly interacting matter in the presence of an external magnetic field has been been explored in model studies and in first principle Lattice Quantum Chromodynamics (LQCD) calculations. These investigations has an importance for physics of heavy-ion collisions at top RHIC and LHC energies, where according to the estimates (see Refs. [1] and [2]), the magnitude of the magnetic field may reach extremely large values of $eB \sim 10 m_\pi^2$.

Model studies (see e.g. Refs. [3–7]) have revealed a general structure of the phase diagram in the temperature-magnetic field ($T - eB$) plane. They showed that the chiral crossover temperature $T_{\rm pc}$ increases with increasing magnetic field. This result has been, however, obtained within a mean-field approximation, i.e. meson fluctuations have not been taken into account. However, charged pion degrees of freedom interacting with the magnetic field may drastically change properties of the crossover transition even at moderate values of B.

Early LQCD calculations [8] confirmed the increase of $T_{\rm pc}$ with eB. Unfortunately, results of Ref. [8] may not be final: the calculations were performed with standard staggered fermions, large lattice spacing and with somewhat heavy pion masses. These deficiencies may diminish the role of charged pions.

Recent LQCD studies [9] at physical pion mass, with improved staggered fermions and extrapolation to the continuum have shown completely opposite dependence of $T_{\rm pc}$ on the magnetic field eB. It has been found that the transition temperature significantly decreases with increasing magnetic field.

In this article, by analysing the chiral structure of the phase diagram of the Polyakov loop-extended quark-meson model beyond a mean-field approximation, we demonstrate, that meson fluctuations cannot explain above mentioned qualitative discrepancy in the behavior of the phase transition temperature with the magnetic field.

LQCD calculations [8] showed that the chiral crossover becomes sharper with the increasing magnetic field. The preliminary results of Ref. [8] indicated that, at a critical end point, the crossover may turn to a first-order phase transition. Our model calculations with physical number of colors $N_c = 3$ show no evidence in favour of possible chiral first-order phase transition in a wide range of the magnetic field. Based on the no-go theorem formulated for QCD in Ref. [10], we will also argue that a chiral critical end point and a change from chiral crossover to a chiral first-order phase transition are forbidden at the leading order of the large N_c expansion for any non-zero pion mass.

In this paper, we do not consider the, so-called, no-sea approximation, the essence of which boils down to neglecting vacuum contributions in a thermodynamic potential. As was shown analytically in Ref. [11], the no-sea approximation results in a first-order chiral phase transition at zero chemical potential in the chiral limit (already on the mean-field level). This is in direct contradiction with recent LQCD findings [12]. We refer to Refs. [3, 13] and [11, 14] for the reader interested in a comparison between results of a properly renormalized theory and those obtained in the no-sea approximation at finite and zero magnetic field correspondingly.

The structure of the paper is as follows. In the next section we discuss the functional renormalization group flow equations in the non-trivial magnetic background. In Section 3, we review the mean-field approximations for the Polyakov loop-extended Quark-Meson (PQM) model. Since the PQM model is renormalizable, we perform dimensional regularization to subtract divergences arising from the vacuum term. Section 4 is devoted to the main results and discussions, including above mentioned input from the large N_c limit. Section 5 contains our conclusions.

*E-Mail:VSkokov@bnl.gov

II. THE POLYAKOV LOOP-EXTENDED QUARK-MESON MODEL

The quark–meson model is an effective realization of the low–energy sector of QCD. The model is built to respect symmetries of QCD, including the chiral symmetry in the limit of vanishing pion mass. However, because the local color $SU(N_c)$ invariance of QCD is replaced by a global symmetry, the model does not describe confinement. The improved version of the model, the so-called Polyakov loop-extended quark-meson (PQM) model incorporates a coupling of the quarks to a uniform temporal color gauge field, represented by the Polyakov loop. In the PQM model, many facets of confinement can be emulated [15–17].

The Lagrangian of the PQM model reads

$$\begin{aligned}\mathcal{L} &= \bar{q}\left[i\gamma^\mu D_\mu - g(\sigma + i\gamma_5 \vec{\tau}\vec{\pi})\right] q \; - \mathcal{U}(\Phi,\Phi^*) \\ &\quad + \frac{1}{2}(\partial_\mu \sigma)^2 + \frac{1}{2}(\partial_\mu \pi^0)^2 + \mathcal{D}_\mu \pi^+ \mathcal{D}^\mu \pi^- - U(\sigma,\vec{\pi}).\end{aligned} \tag{1}$$

The coupling between the effective gluon field and quarks, and between the (electro)magnetic field B and quarks is implemented through the covariant derivative

$$D_\mu = \partial_\mu - iA_\mu - iQA_\mu^{\mathrm{EM}}, \tag{2}$$

where $A_\mu = g\,A_\mu^a\,\lambda^a/2$ and $A_\mu^{\mathrm{EM}} = (0, Bx, 0, 0)$. The flavor matrix Q is defined by the quark electric charges $Q = \mathrm{diag}(2/3e, -1/3e)$. The spatial components of the gluon field are neglected, i.e. $A_\mu = \delta_{\mu 0} A_0$. The interaction of charged pion $\pi^\pm = (\pi_1 \pm i\pi_2)/\sqrt{2}$ with the electromagnetic field is included by $\mathcal{D}_\mu = \partial_\mu + ieA_\mu^{\mathrm{EM}}$. The effective potential for the gluon field $\mathcal{U}(\Phi,\Phi^*)$ is expressed in terms of the thermal expectation values of the color trace of the Polyakov loop and its conjugate

$$\Phi = \frac{1}{N_c}\langle \mathrm{Tr}_c L(\vec{x})\rangle, \quad \Phi^* = \frac{1}{N_c}\langle \mathrm{Tr}_c L^\dagger(\vec{x})\rangle, \tag{3}$$

with

$$L(\vec{x}) = \mathcal{P}\exp\left[i\int_0^\beta d\tau A_4(\vec{x},\tau)\right], \tag{4}$$

where $\mathcal{P}$ stands for the path ordering, $\beta = 1/T$ and $A_4 = i\,A_0$. In the $O(4)$ representation, the meson field is introduced as $\phi = (\sigma, \vec{\pi} = (\pi_0, \pi_1, \pi_2))$ and the corresponding $SU(2)_L \otimes SU(2)_R$ chiral representation is defined by $\sigma + i\vec{\tau}\cdot\vec{\pi}\gamma_5$.

The meson potential of the model, $U(\sigma,\vec{\pi})$, is defined as

$$U(\sigma,\vec{\pi}) = \frac{\lambda}{4}\left(\sigma^2 + \vec{\pi}^2 - v^2\right)^2 - c\sigma. \tag{5}$$

The effective potential of the gluon field is parametrized in such a way as to preserve the $Z(3)$ invariance:

$$\frac{\mathcal{U}(\Phi,\Phi^*)}{T^4} = -\frac{b_2(T)}{2}\Phi^*\Phi - \frac{b_3}{6}(\Phi^3 + \Phi^{*3}) + \frac{b_4}{4}(\Phi^*\Phi)^2\,. \tag{6}$$

The parameters,

$$b_2(T) \;=\; a_0 + a_1\left(\frac{T_0}{T}\right) + a_2\left(\frac{T_0}{T}\right)^2 + a_3\left(\frac{T_0}{T}\right)^3 \tag{7}$$

with $a_0 = 6.75$, $a_1 = -1.95$, $a_2 = 2.625$, $a_3 = -7.44$, $b_3 = 0.75$, $b_4 = 7.5$ and $T_0 = 270$ MeV were chosen to reproduce the equation of state of the pure $\mathrm{SU}_c(3)$ lattice gauge theory. When the coupling to the quark degrees of freedom are neglected, the potential (6) yields a first-order deconfinement phase transition at T_0.

A. The FRG method in the PQM model

To take fluctuations into account in the PQM model, we use the functional renormalization group (FRG) method. This method is based on an infrared regularization of the fluctuations at a sliding momentum scale k, resulting in a scale-dependent effective action Γ_k, the so-called effective average action [18]. In this article, the Polyakov loop is treated as a background field introduced self-consistently on the mean-field level. Quark and meson fluctuations are accounted for by solving the FRG flow equations.

The FRG flow equation for the PQM model at zero magnetic field was derived in Ref. [19]. The derivation for finite magnetic field is lengthy, but straightforward and can be done along similar lines. Here we provide only the final expression for the flow equation. It can be easily proved that in the limit $B \to 0$ the flow equation reduces to that of Ref. [19].

Following our previous work [19], the flow equation for the scale-dependent grand canonical potential density,

$\Omega_k = T\Gamma_k/V$, is formulated for the quark and meson subsystems in the leading order of derivative expansion

$$\partial_k\Omega_k(\Phi,\Phi^*;T,\mu) = \frac{k^4}{12\pi^2}\left\{\left[\frac{1+2n_B(E_\pi;T)}{E_\pi}\right]+\left[\frac{1+2n_B(E_\sigma;T)}{E_\sigma}\right]\right\} \tag{8}$$
$$+k\frac{eB}{2\pi^2}\sum_{n=0}^{\infty}\sqrt{k^2-q_\perp^2(n,e,0)}\theta(k^2-q_\perp^2(n,e,0))\left[\frac{1+2n_B(E_\pi;T)}{E_\pi}\right]$$
$$-k\sum_{f=1,2}\frac{N_cQ_{ff}B}{2\pi^2}\sum_{s=\frac{1}{2},-\frac{1}{2}}\sum_{n=0}^{\infty}\sqrt{k^2-q_\perp^2(n,Q_{ff},s)}\theta(k^2-q_\perp^2(n,Q_{ff},s))\left[\frac{1-N(\Phi,\Phi^*;T,\mu)-\bar{N}(\Phi,\Phi^*;T,\mu)}{E_q}\right].$$

Here $n_B(E_{\pi,\sigma};T)$ is the bosonic distribution function

$$n_B(E_{\pi,\sigma};T) = \frac{1}{\exp(E_{\pi,\sigma}/T)-1},$$

with the pion and sigma energies

$$E_\pi = \sqrt{k^2+\overline{\Omega}_k'}\ \ ,\ E_\sigma = \sqrt{k^2+\overline{\Omega}_k'+2\rho\,\overline{\Omega}_k''},$$

where the primes denote derivatives with respect to $\rho=(\sigma^2+\vec{\pi}^2)/2$ of $\overline{\Omega}=\Omega+c\sigma$. The fermion distribution functions $N(\Phi,\Phi^*;T,\mu)$ and $\bar{N}(\Phi,\Phi^*;T,\mu)$,

$$N(\Phi,\Phi^*;T,\mu) = \frac{1+2\Phi^*\exp[\beta(E_q-\mu)]+\Phi\exp[2\beta(E_q-\mu)]}{1+3\Phi\exp[2\beta(E_q-\mu)]+3\Phi^*\exp[\beta(E_q-\mu)]+\exp[3\beta(E_q-\mu)]}, \tag{9}$$
$$\bar{N}(\Phi,\Phi^*;T,\mu) = N(\Phi^*,\Phi;T,-\mu), \tag{10}$$

are modified because of the coupling to the gluon field. The quark energy is given by

$$E_q = \sqrt{k^2+2g^2\rho}. \tag{11}$$

The function $q_\perp^2$ is defined as $q_\perp^2(n,q,s)=(2n+1-2s)|q|B$ and has the same structure as in mean-field approximation, see Ref. [3].

If one replaces the energies of particles by their tree-level approximation and integrate the flow equation with respect to the scale k, then, after integration by parts, the effective thermodynamic potential Ω reduces to the one-loop result for the PQM model in the presence of non-zero magnetic field. This also proves validity of the flow equation (8).

The minimum of the thermodynamic potential is determined by the stationarity condition

$$\left.\frac{d\Omega_k}{d\sigma}\right|_{\sigma=\sigma_k} = \left.\frac{d\overline{\Omega}_k}{d\sigma}\right|_{\sigma=\sigma_k} - c = 0. \tag{12}$$

We solve the flow equation (8) numerically with the initial cutoff $\Lambda = 1.2$ GeV (see additional details in Ref. [19]). The initial conditions for the flow are fixed to reproduce the in-vacuum properties ($T=\mu=0$, $eB=0$) : the physical pion mass $m_\pi = 138$ MeV, the pion decay constant $f_\pi = 93$ MeV, the sigma mass $m_\sigma = 600$ MeV, and the constituent quark mass $m_q = 300$ MeV at the scale $k\to 0$. We treat the symmetry breaking term, $c = m_\pi^2 f_\pi$ as an external field. We also neglect the flow of the Yukawa coupling g, which is not expected to be significant for the present studies (see e.g. Refs. [20, 21]).

The thermodynamic potential (13) does not contain contributions of thermal modes with momenta larger than the cutoff Λ. To obtain the correct high-temperature behavior of thermodynamic functions we need to supplement the FRG potential with the contribution of the high-momentum states. For this, we follow the procedure described in Ref. [19]: at high $k>\Lambda$ the meson contribution to the flow in the equation is disregarded and only the flow of massless quarks interacting with the Polyakov loop is considered.

By solving Eq. (8), one obtains the thermodynamic potential for the quark and meson subsystems, $\Omega_{k\to 0}(\Phi,\Phi^*;T,\mu)$, as a function of the Polyakov loop variables Φ and Φ^*. The full thermodynamic potential $\Omega(\Phi,\Phi^*;T,\mu)$ in the PQM model, including quark, meson and gluon degrees of freedom, is obtained by adding the effective gluon potential $\mathcal{U}(\Phi,\Phi^*)$ to $\Omega_{k\to 0}(\Phi,\Phi^*;T,\mu)$:

$$\Omega(\Phi,\Phi^*;T,\mu) = \Omega_{k\to 0}(\Phi,\Phi^*;T,\mu)+\mathcal{U}(\Phi,\Phi^*). \tag{13}$$

The Polyakov loop variables, Φ and Φ^*, are then deter-

mined by the stationarity conditions:

$$\frac{\partial}{\partial\Phi}\Omega(\Phi,\Phi^*;T,\mu)=0, \tag{14}$$

$$\frac{\partial}{\partial\Phi^*}\Omega(\Phi,\Phi^*;T,\mu)=0. \tag{15}$$

B. The mean-field approximation

To illustrate the importance of meson fluctuations on the thermodynamics of the PQM model we compare the FRG results with those obtained in the mean-field approximation. As we earlier alluded to the one-loop thermodynamic potential, the mean-field approximation can be also directly obtained from the flow equation (8) by
(i) neglecting fluctuations of the meson fields and replacing them by their classical expectation values;
(ii) integrating the flow equation with respect to the scale k;
(iii) performing integration by parts;
(iv) and, finally, by minimizing the thermodynamical potential with respect to the mean fields.

In this way, we will obtain the thermodynamical potential for the PQM model in the mean-field approximation, which coincides with the direct mean-field treatment (see Ref. [3]) for the Lagrangian (1):

$$\Omega_{\rm MF}=\mathcal{U}(\Phi,\Phi^*)+U(\langle\sigma\rangle,\langle\pi\rangle=0)+\Omega_{q\bar{q}}(\langle\sigma\rangle,\Phi,\Phi^*). \tag{16}$$

Here, the contribution of quarks with the dynamical mass $m_q=g\langle\sigma\rangle$ is given by

$$\Omega_{q\bar{q}}(\langle\sigma\rangle,\Phi,\Phi^*)=-T\sum_{f=1,2}\sum_{s=-\frac{1}{2},\frac{1}{2}}\sum_{n=0}^{\infty}\frac{|Q_{ff}|B}{2\pi}\int\frac{dp_z}{2\pi}\left\{\frac{N_cE_q}{T}+\ln g^{(+)}(\langle\sigma\rangle,\Phi,\Phi^*;T,\mu)+\ln g^{(-)}(\langle\sigma\rangle,\Phi,\Phi^*;T,\mu)\right\}, \tag{17}$$

where

$$g^{(+)}(\langle\sigma\rangle,\Phi,\Phi^*;T,\mu) = 1+3\Phi\exp[-(E_q-\mu)/T]+3\Phi^*\exp[-2(E_q-\mu)/T]+\exp[-3(E_q-\mu)/T], \tag{18}$$

$$g^{(-)}(\langle\sigma\rangle,\Phi,\Phi^*;T,\mu) = g^{(+)}(\langle\sigma\rangle,\Phi^*,\Phi;T,-\mu) \tag{19}$$

and $E_q=\sqrt{p_3^2+q_\perp^2(n,Q_{ff},s)+m_q^2}$ is the quark quasi-particle energy (see the definition of $q_\perp^2$ in the previous section). The first term in Eq. (17) is a divergent vacuum fluctuation contribution, which has to be properly regularized. Following Refs. [11] and [3], we employ dimensional regularization to obtain:

$$\Omega_{q\bar{q}}^{\rm vac(B)}=-\frac{N_c}{2\pi^2}\sum_{f=1,2}(Q_{ff}B)^2\left[\frac{x_f}{2}\ln x_f+\frac{x_f^2}{2}\ln\frac{2|Q_{ff}|B}{M^2}+\frac{x_f^2}{4}+\zeta'(-1,x_f)\right], \tag{20}$$

where M is the renormalization scale, $x_f=m_q^2/(2|Q_{ff}B|)$ and $\zeta(t,x)$ is the Hurwitz zeta function.

In Eq. (20) the prime denotes the derivative with respect to the first argument $\zeta'(t,x)=\partial\zeta(t,x)/\partial t$. The divergent contribution were subtracted from Eq. (20) to reproduce $B\to 0$ result for the vacuum contribution [11]

$$\Omega_{q\bar{q}}^{\rm vac}=-\frac{N_cN_f}{8\pi^2}m_q^4\ln\left(\frac{m_q}{M}\right). \tag{21}$$

Indeed, using the asymptotic expansion of $\zeta'(-1,x_f)$ in the limit $B\to 0$ or equivalently $x_f\to\infty$ (see Ref. [22])

$$\zeta'(-1,x_f)\approx\frac{1}{2}\left[x_f^2-x_f+\frac{1}{6}\right]\ln x_f-\frac{x_f}{4}+\frac{1}{12}+O(x_f^{-1}) \tag{22}$$

it is easy to prove that $\lim_{B\to0}\Omega_{q\bar{q}}^{\rm vac(B)}=\Omega_{q\bar{q}}^{\rm vac}$.

In case of $eB=0$, the relevance of the vacuum contribution for the thermodynamics of chiral models was demonstrated and studied in detail in Refs. [11] and [23].

As usual, the equations of motion for the mean fields are obtained by requiring that the thermodynamic potential is stationary with respect to changes of $\langle\sigma\rangle$, Φ and Φ^*:

$$\frac{\partial\Omega_{\rm MF}}{\partial\langle\sigma\rangle}=\frac{\partial\Omega_{\rm MF}}{\partial\Phi}=\frac{\partial\Omega_{\rm MF}}{\partial\Phi^*}=0. \tag{23}$$

The derivative of the thermodynamic potential with respect to the chiral order parameter σ also involves $\partial\zeta'(-1,x_f)/\partial x_f$ which is given by

$$\frac{\partial\zeta'(-1,x_f)}{\partial x_f}=x-\frac{1}{2}+\ln\frac{\Gamma(x)}{\sqrt{2\pi}}. \tag{24}$$

The model parameters are fixed to reproduce the same vacuum physics as in the FRG calculation.

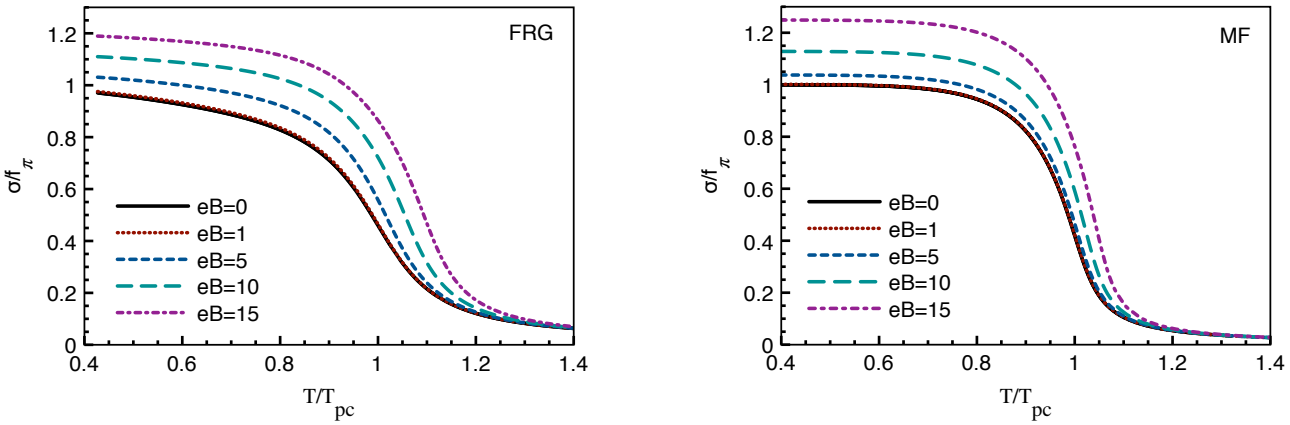

FIG. 1: The chiral order parameter as a function of the temperature for the different values of the magnetic field eB measured in units of m_π^2. The left (right) panel shows the FRG (mean-field) results.

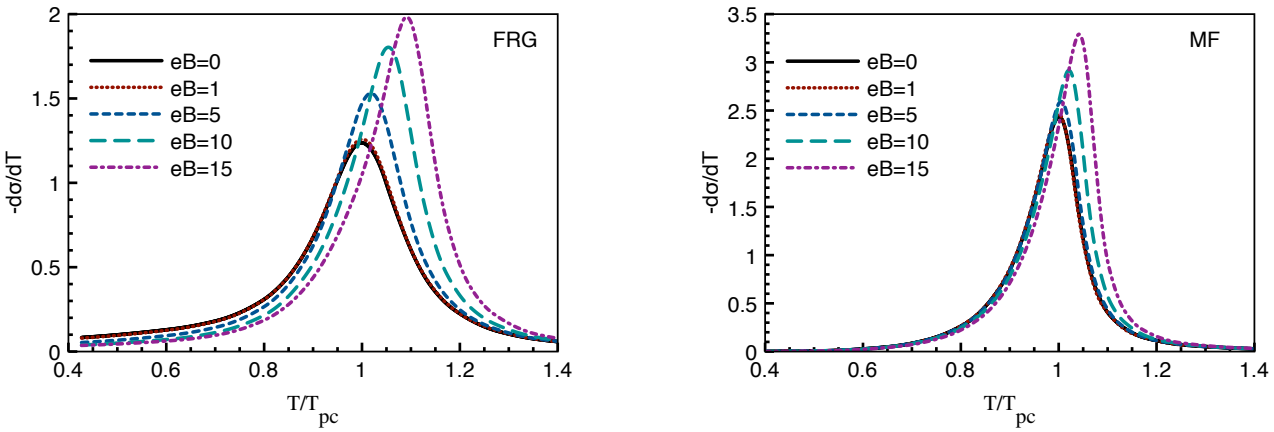

FIG. 2: The derivative of the order parameter with respect to T as a function of the temperature for the different values of the magnetic field eB measured in units of m_π^2. The left (right) panel shows the FRG (mean-field) results.

III. PHASE DIAGRAM IN THE $T - eB$ PLANE

In this section, we explore the properties of the chiral crossover transition at finite temperature T and magnetic field eB in the functional renormalization group (FRG) approach and in the mean-field approximation for the PQM model. The comparison of the results in two approaches allows to pin down the role of meson fluctuations. As our calculations show meson fluctuations lead to even steeper rise of the transition temperature with increasing field and, thus, are unable to describe the qualitative discrepancy between recent LQCD results [9] and the mean-field model predictions, which have been qualitatively confirmed in early LQCD calculations [8].

In the FRG approach, the thermodynamic potential (13) at finite temperature and chemical potential is obtained by solving the flow equation (8) numerically, using the Taylor expansion method (for details see Ref. [19] and references therein). This approach has been successful applied to the thermodynamics at finite density and temperature [19, 23].

The structure of the chiral phase diagram can be revealed by investigating the chiral order parameter σ. In Fig. 1, the dependence of the order parameter on the temperature normalized by $T_{\rm pc}$ [34] for different values of the magnetic field eB is shown in the FRG approach and the mean-field approximation. Our results are in agreement with those of Refs. [19, 24] at zero magnetic field and lead to the same conclusion: meson fluctuations result in a strong smearing of the temperature dependence of the order parameter, decreasing the strength of the transition. By considering the derivative of the order parameter with respect to the temperature, see Fig. 2., we conclude that the transition in both models shifts to higher temperatures with increasing magnetic field. Figure 2 also demonstrates that the strength of the transition characterized by the peak in $|d\sigma/dT|$ increases slightly with magnetic field. This increase is minute for the mean-field approximation and more pronounced if meson fluctuations are taken into account by the FRG approach.

The same conclusion on the minor modification of the

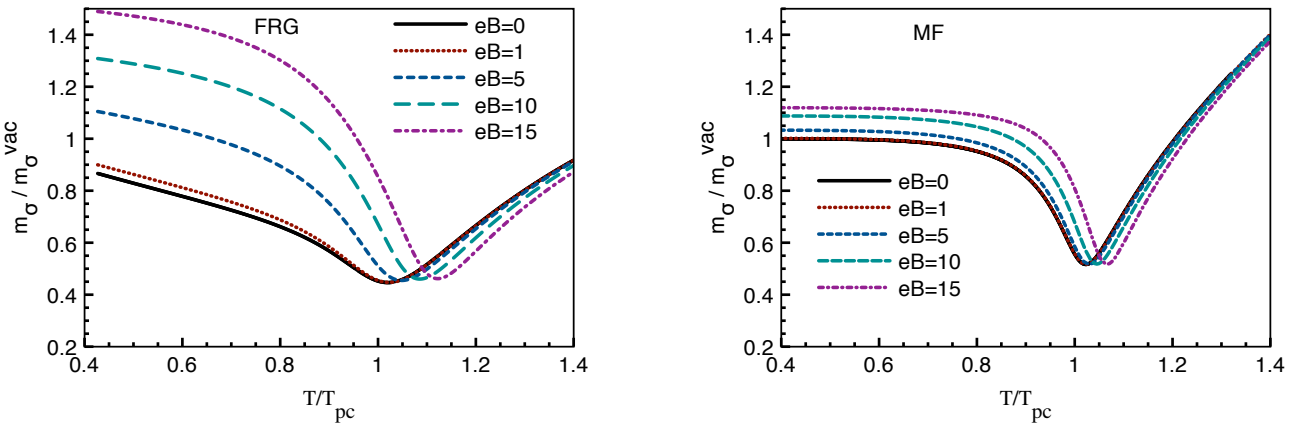

FIG. 3: The mass of the σ as a function of the temperature for the different values of the magnetic field eB measured in units of m_π^2. The left (right) panel shows the FRG (mean-field) results.

transition strength follows from Fig. 3, where the mass of σ-meson as a function of temperature and magnetic field is shown. Figure 3 demonstrates, that in the FRG approach, the mass of σ-meson in the broken phase is modified by the magnetic field stronger than the one in the mean-field approach. This is expected because the charged meson fluctuations included in FRG make the σ mass more sensitive to the magnetic field.

At the chiral critical end point, the mass of σ-meson (order parameter) is vanishing $m_\sigma \to 0$. Consequently, σ mass decreases along the crossover line towards the critical end point in the $T-\mu_B$ plane. Contrary to this at zero μ_B and non-zero magnetic field eB, we do not observe this trend. In both approaches, the value of σ mass at the minimum is almost independent of the magnetic field. We checked this fact up to very high magnitudes of the magnetic field $eB = 30m_\pi^2$. Based on this observation, possible chiral critical end point in the PQM model can be excluded in a very wide range of the magnetic field [35]. After considering the phase diagram in the $T-eB$ plane, we will return to this problem again addressing it from a different side.

By locating the maximum of the peak position in $|d\sigma/dT|$ as a function of T at a given B we compute the phase diagram of the chiral crossover transition in the $T-eB$ plane. The phase diagram is shown in Fig. 4. Contrary to the recent lattice findings [9], the slope of the transition line, ξ, is positive. The inclusion of meson fluctuation increases the slope calculated at large values of the magnetic field from $\xi_{\rm MF} \approx 4.7 \cdot 10^{-3}$ to $\xi_{\rm FRG} \approx 7.1 \cdot 10^{-3}$. Performing the parametrization

$$\frac{T_{pc}(B)}{T_{\rm pc}} = 1 + A\left(\frac{eB}{T_{\rm pc}^2}\right)^\alpha \qquad (25)$$

of the phase transition line, which was introduced in Ref. [8], we obtain $\alpha_{\rm MF} = 6 \cdot 10^{-4}$ in the mean-field approximation and $\alpha_{\rm FRG} = 2.7 \cdot 10^{-3}$ in the FRG approach. In the PQM model, the role of meson fluctuations at a finite magnetic field may be understood by the following considerations. At zero magnetic field, the meson contribution to the flow at any temperatures (including $T=0$) reduces the chiral condensate, i.e. works towards the chiral restoration. At a finite magnetic field, the charged pions acquire an additional effective mass proportional to eB, which penalizes meson contribution to the restoration of the chiral symmetry at non-zero magnetic field. The quark contribution is not that trivial for analytic considerations: while the finite temperature part acts towards the restoration of the chiral symmetry, the vacuum part has an opposite effect. The numerical mean-field calculations show that the quark contribution increases the transition temperature.

Another interesting issue that can be studied in LQCD calculations and that may shed light to the QCD phase diagram in the three dimensional $T-eB-\mu_B$ space is the curvature of the crossover transition line in $T-\mu_B$ plane κ for non-zero magnetic field. The curvature is defined by

$$\frac{T_{\rm pc}(B,\mu_B)}{T_{\rm pc}(B,\mu_B=0)} = 1+\kappa(B)\left(\frac{\mu_B}{T}\right)^2+\mathcal{O}\left(\left[\frac{\mu_B}{T}\right]^4\right). \qquad (26)$$

In Fig. 5, we show the curvature of the crossover line $\kappa(B)$ normalized by its value at zero magnetic field $\kappa_0 = \kappa(B=0)$ [36]. The curvature in the FRG approach at higher magnetic field shows stronger dependence.

The issue of the chiral critical end point and subsequent chiral first-order phase transition in the $T-eB$ plane can be addressed by a completely different approach of the QCD inequalities developed in Refs. [25–28] and recently discussed in Ref. [10]. Background electromagnetic field does not break neither positivity of the Dirac operator ($\mathcal{D}$) nor its γ_5-hermiticity [37] ($\gamma_5\mathcal{D}\gamma_5 = \mathcal{D}^\dagger$). Thus the results of Ref. [10] can be with no modification extended to the case of the non-zero magnetic field. The QCD inequalities [25–28] can be translated to those for the meson masses $m_\alpha \geq m_\pi$, where m_π is the mass of the lightest pseudoscalar pion and m_α is the lightest meson mass in the channel α,

consult Ref. [10] for details. This inequality is rigorous for non flavor singlet α. In the large N_c limit, however, owing to $1/N_c$ suppression of the flavor disconnected diagrams, this inequality becomes applicable for flavor singlet channel too. For us it is essential, that $m_\sigma \geq m_\pi$ at the leading order of large N_c expansion. From the last inequality, it follows that at any finite value of the pion mass the correlation length proportional to $1/m_\sigma$ is finite, i.e. the chiral second-order phase transition is impossible. For the sake of argument, we remind the reader that it has been rigorously established in high precision LQCD calculations of different groups [29–31] that for the physical pion mass and at zero magnetic field and $T \approx 155$ MeV [31, 32] the chiral transition is a smooth crossover. In principle, the chiral crossover transition may turn into the first-order one at a finite value of the magnetic field. This, however, may happen only via second-order critical end point. The above mentioned argument disfavours such possibility at least in the large N_c limit.

We note, however, that this argument applies only to the chiral transition. Existence of other phase transitions (e.g. the first-order deconfinement phase transition) at high eB cannot be excluded.

IV. SUMMARY AND CONCLUSIONS

Results of the recent LQCD calculations on the dependence of the transition temperature on the magnetic field disagree already at a qualitative level with those obtained previously, as well as with various low energy effective model of QCD. In this article, we addressed this issue in the Polyakov loop-extended quark-meson model beyond the mean-field approximation. We showed that the inclusion of meson fluctuations, which presumable were suppressed in the early LQCD fluctuations and were neglected in the mean-field models, is unable to resolve the above mentioned disagreement.

We calculated the phase diagram of the Polyakov loop-extended quark-meson model in the mean-field approximation and in the functional renormalization group approach. Both approaches result in a shift of the transition temperatures to higher values then that at zero magnetic field. Moreover, the relative increase of the transition temperature is larger if meson fluctuations are taken into account.

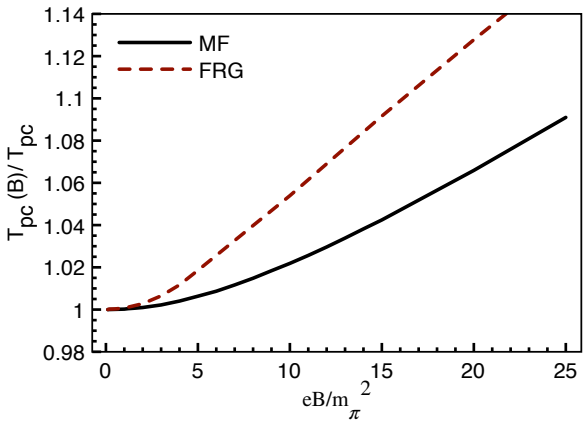

FIG. 4: The phase diagram in the FRG approach and mean-field approximation.

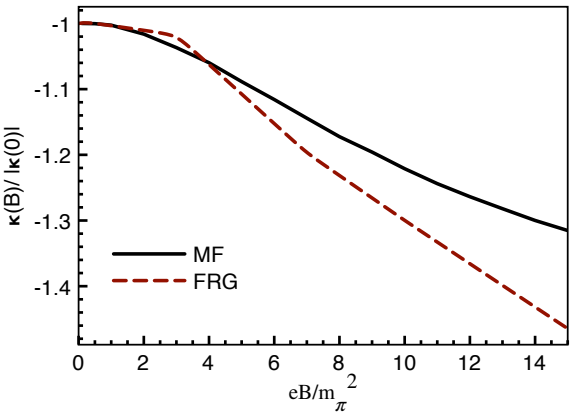

FIG. 5: The curvature of the transition line in $T-\mu_B$ plane, κ, as a function of the magnetic field.

Although we observed that the transition strength increases with increasing magnetic field, we see no evidence in favour of possible chiral first-order phase transition at finite values of the magnetic field eB.

Based on the large N_c non-go theorem of Ref. [10], we provide another indication against a chiral critical end point and a change from the chiral crossover to a first-order phase transition in the $T-eB$ plane for non-zero pion mass.

Finally, in the PQM model calculations, it was also shown that the magnetic field increases the curvature of the transition in the $T-\mu_B$ plane.

In this article, we restricted ourselves to zero baryon chemical potential. Nonetheless, the FRG approach to the PQM model at a finite magnetic field can be successfully applied at finite densities.

In this model, we do not take into account a contribution of the charged vector mesons, e.g. $\rho^\pm$. As was shown in Ref. [33], in a high magnetic field ($eB_c \approx m_\rho^2$), the ρ-meson condensate may form and drastically change properties of nuclear matter.

Acknowledgments

The FRG approach to the PQM model at zero magnetic field has been developed in collaboration with B. Friman and K. Redlich. I am grateful to them for illuminating discussions on many aspects of the functional renormalization group approach and its application to thermodynamics.

I thank S. Mukherjee and R. Pisarski for useful discus-

sions. Many helpful comments by A. Bzdak, B. Friman and K. Morita are acknowledged.

I also thank N. Yamamoto for his clear explanation of the QCD inequalities during his seminar at BNL.

This manuscript has been authorized under Contract No. DE-AC02-98H10886 with the U. S. Department of Energy.

[1] D. E. Kharzeev, L. D. McLerran and H. J. Warringa, Nucl. Phys. A **803**, 227 (2008).
[2] V. Skokov, A. Y. Illarionov and V. Toneev, Int. J. Mod. Phys. A **24**, 5925 (2009); A. Bzdak and V. Skokov, arXiv:1111.1949 [hep-ph].
[3] A. J. Mizher, M. N. Chernodub and E. S. Fraga, Phys. Rev. D **82**, 105016 (2010).
[4] C. V. Johnson and A. Kundu, JHEP **0812**, 053 (2008).
[5] E. S. Fraga and A. J. Mizher, Nucl. Phys. A **820**, 103C (2009).
[6] R. Gatto and M. Ruggieri, Phys. Rev. D **83**, 034016 (2011).
[7] R. Gatto and M. Ruggieri, Phys. Rev. D **82**, 054027 (2010).
[8] M. D'Elia, S. Mukherjee and F. Sanfilippo, Phys. Rev. D **82**, 051501 (2010).
[9] G. S. Bali *et al.*, arXiv:1111.4956 [hep-lat].
[10] Y. Hidaka and N. Yamamoto, arXiv:1110.3044 [hep-ph].
[11] V. Skokov, B. Friman, E. Nakano, K. Redlich and B. J. Schaefer, Phys. Rev. D **82**, 034029 (2010).
[12] S. Ejiri *et al.*, Phys. Rev. D **80**, 094505 (2009).
[13] J. O. Andersen and R. Khan, arXiv:1105.1290 [hep-ph].
[14] J. O. Andersen, R. Khan and L. T. Kyllingstad, arXiv:1102.2779 [hep-ph].
[15] K. Fukushima, Phys. Lett. B **591**, 277 (2004).
[16] C. Ratti, M. A. Thaler and W. Weise, Phys. Rev. D **73**, 014019 (2006).
[17] B. J. Schaefer, J. M. Pawlowski and J. Wambach, Phys. Rev. D **76**, 074023 (2007).
[18] J. Berges, N. Tetradis and C. Wetterich, Phys. Rept. **363**, 223 (2002).
[19] V. Skokov, B. Stokic, B. Friman and K. Redlich, Phys. Rev. C **82**, 015206 (2010)
[20] D. U. Jungnickel and C. Wetterich, Phys. Rev. D **53**, 5142 (1996).
[21] J. Berges, D. U. Jungnickel and C. Wetterich, Phys. Rev. D **59**, 034010 (1999).
[22] S. Rudaz, J. Math. Phys. **31**, 2832 (1990).
[23] E. Nakano, B. J. Schaefer, B. Stokic, B. Friman and K. Redlich, Phys. Lett. **B682**, 401 (2010).
[24] K. Morita, V. Skokov, B. Friman and K. Redlich, Phys. Rev. D **84**, 074020 (2011).
[25] D. Weingarten, Phys. Rev. Lett. **51**, 1830 (1983).
[26] E. Witten, Phys. Rev. Lett. **51**, 2351 (1983).
[27] S. Nussinov, Phys. Rev. Lett. **52**, 966 (1984).
[28] D. Espriu, M. Gross and J. F. Wheater, Phys. Lett. B **146**, 67 (1984).
[29] C. Bernard *et al.* [MILC Collaboration], Phys. Rev. D **71**, 034504 (2005).
[30] M. Cheng *et al.*, Phys. Rev. D **74**, 054507 (2006).
[31] Y. Aoki, G. Endrodi, Z. Fodor, S. D. Katz and K. K. Szabo, Nature **443**, 675 (2006).
[32] A. Bazavov *et al.*, arXiv:1111.1710 [hep-lat].
[33] M. N. Chernodub, Phys. Rev. Lett. **106**, 142003 (2011).
[34] The transition temperature T_{pc} is defined as a position of the maximum in $|d\sigma/dT|$ at zero magnetic field. In the FRG approach and in the mean-fied approximation we have $T_{\rm pc}^{\rm FRG} \approx 234$ MeV and $T_{\rm pc}^{\rm MF} \approx 227$ MeV.
[35] We note that this is not a universal property and might be different in QCD. See also the discussion on QCD in the large N_c limit at the end of this section.
[36] The curvature of the phase transition in the $T-\mu_B$ plane at zero magnetic field is given by $\kappa_{\rm MF}(B=0) \approx -0.156$ for the mean-field approximation, $\kappa_{\rm FRG}(B=0) \approx -0.17$ for the FRG approach.
[37] In contrast to the baryon chemical potential.